

SERN: Simulation-Enhanced Realistic Navigation for Multi-Agent Robotic Systems in Contested Environments

Jumman Hossain¹, Emon Dey¹, Snehalraj Chugh¹, Masud Ahmed¹, MS Anwar¹, Abu-Zaher Faridee^{1,2}, Jason Hoppes³, Theron Trout³, Anjon Basak³, Rafidh Chowdhury³, Rishabh Mistry³, Hyun Kim³, Jade Freeman⁴, Niranjan Suri⁴, Adrienne Raglin⁴, Carl Busart⁴, Timothy Gregory⁴, Anuradha Ravi¹, and Nirmalya Roy¹

Abstract—The increasing deployment of autonomous systems in complex environments necessitates efficient communication and task completion among multiple agents. This paper presents SERN (Simulation-Enhanced Realistic Navigation), a novel framework integrating virtual and physical environments for real-time collaborative decision-making in multi-robot systems. SERN addresses key challenges in asset deployment and coordination through our bi-directional SERN ROS Bridge communication framework. Our approach advances the SOTA through: accurate real-world representation in virtual environments using Unity high-fidelity simulator; synchronization of physical and virtual robot movements; efficient ROS data distribution between remote locations; and integration of SOTA semantic segmentation for enhanced environmental perception. Additionally, we introduce a Multi-Metric Cost Function (MMCF) that dynamically balances latency, reliability, computational overhead, and bandwidth consumption to optimize system performance in contested environments. We further provide theoretical justification for synchronization accuracy by proving that the positional error between physical and virtual robots remains bounded under varying network conditions. Our evaluations show a 15% to 24% improvement in latency and up to a 15% increase in processing efficiency compared to traditional ROS setups. Real-world and virtual simulation experiments with multiple robots (Clearpath Jackal and Husky) demonstrate synchronization accuracy, achieving less than 5 cm positional error and under 2° rotational error. These results highlight SERN’s potential to enhance situational awareness and multi-agent coordination in diverse, contested environments.

I. INTRODUCTION

The deployment of autonomous multi-robot systems in real-world environments presents significant challenges, including the need for robust communication, real-time synchronization, and adaptive decision-making. As these systems increasingly operate in complex, dynamic, and often contested environments—ranging from urban areas to disaster sites—there is a growing need for frameworks that can seamlessly integrate virtual simulations with physical deployments [1]–[3]. Such integration enables more effective testing, planning, and execution, allowing robots to leverage both simulated predictions and real-world feedback to enhance their operational efficiency [4].

Project Page: <https://pralgomathic.github.io/sern.multi-agent/>

*This work has been partially supported by ONR Grant #N00014-23-1-2119, U.S. Army Grant #W911NF2120076, U.S. Army Grant #W911NF2410367, NSF REU Site Grant #2050999, NSF CNS EAGER Grant #2233879, and NSF CAREER Award #1750936.

¹Department of Information Systems, University of Maryland, Baltimore County, USA. {jumman.hossain, edey1, schugh1, mahmed10, nroy}@umbc.edu.

²Amazon Inc., USA. abufari@amazon.com.

³Stormfish Scientific Corporation, theron.trout@stormfish-sci.com.

⁴DEVCOM Army Research Lab, USA.

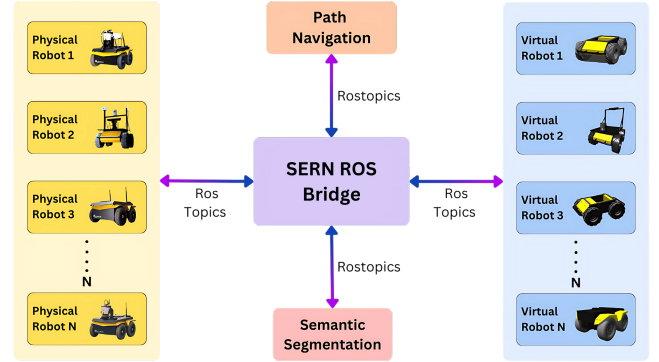


Fig. 1: SERN framework implementation demonstrating bi-directional communication between physical and virtual robots. The system enables synchronized path planning and cross-domain data sharing across separate physical and virtual networks, supporting coordinated multi-robot operations.

Traditional approaches to robot navigation and coordination often rely on either purely virtual simulations or physical trials, each with inherent limitations [5]–[7]. Virtual simulations can offer predictive insights but often lack the fidelity needed for accurate real-world replication, while physical trials can be costly, time-consuming, and limited in scope [8]. Bridging the gap between these two domains has the potential to significantly enhance the performance of multi-agent systems by combining the strengths of both approaches [1], [9]. However, existing frameworks face challenges such as high latency in data synchronization, inefficient communication protocols, and difficulties in maintaining consistent situational awareness across distributed environments [2], [6], [10].

To address these challenges, we introduce SERN (Simulation-Enhanced Realistic Navigation), a novel framework designed to integrate virtual and physical environments seamlessly (Fig. 1). SERN provides an adaptive bi-directional communication infrastructure that reduces latency and optimizes data flow, ensuring that both virtual and physical agents operate with synchronized situational awareness [5], [11]. By incorporating a physics-based synchronization model and semantic-aware ROS topic management, SERN improves the fidelity of virtual-to-physical transitions and enhances the overall coordination among robotic agents [6], [12]. The main contributions of our work are:

- **Integrated Virtual-Physical Environment Represent-**

tation: We present a novel approach for accurate real-world representation in virtual environments using Unity’s high-fidelity simulator [13]. Our method incorporates geospatial data and adaptive modeling techniques, significantly reducing the time and effort associated with traditional manual terrain modeling.

- **SERN ROS Bridge for Distributed Communication:** While AuroraXR [14] was originally built for cross-reality data exchange, we significantly extend it to meet multi-robot system demands. We introduce a semantic prioritization layer for bandwidth-constrained networks, a dynamic topic discovery mechanism for newly added robots, and a fault-tolerant messaging protocol that buffers and replays data to preserve group coordination during disruptions. These enhancements, built atop a custom ZeroMQ pipeline, yield 15–24% lower latency compared to standard ROS networking under equivalent loads. Far from simply reusing existing software, we refine AuroraXR [14] into an extensible communication backbone for large-scale multi-agent robotics operating in contested environments.
- **Physics-Aware Synchronization of Robot Movements:** We introduce a dynamic modeling approach for synchronizing physical and virtual robot movements. Our method incorporates key physical parameters and a PD control strategy, achieving an average positional error of less than 5cm and rotational error under 2° between physical and virtual robots.
- **Scalable Multi-Agent Coordination:** We demonstrate the scalability of SERN through extensive experiments involving various numbers of robots, showing robust performance improvements in scenarios that reflect real-world operational challenges. SERN’s design supports the deployment of large-scale multi-agent systems, maintaining system integrity and synchronization accuracy even as the number of participating agents increases.
- **Multi-Metric Cost Function (MMCF):** We introduce a comprehensive optimization framework that balances competing objectives (latency, reliability, computational overhead, and bandwidth) through a weighted cost function. This allows SERN to make optimal configuration decisions that reflect mission-specific priorities while achieving 37% lower overall operational cost compared to fixed configurations.
- **Cross-Domain Semantic Segmentation and Navigation:** We implement a domain adaptation-based approach for semantic segmentation, leveraging 3D LiDAR data to enhance generalization across different environments. This is integrated with a navigation system that operates seamlessly in both physical and virtual domains, demonstrating improved path planning and obstacle avoidance.

Experiments demonstrate SERN’s performance in complex scenarios. Compared to traditional ROS systems, our evaluations show a 15% to 24% improvement in latency and up to a 15% increase in processing efficiency, with results

indicating improved network performance (46.9% to 54.5% latency reduction), scalability, and synchronization accuracy (< 5 cm positional error, $< 2^\circ$ rotational error).

II. RELATED WORK

In this section, we address existing challenges in real-time communication, synchronization, and multi-robot coordination during navigation between virtual and physical robotics.

A. Synchronizing Physical and Virtual Domains with Real-Time Communication

Efficient bidirectional communication and real-time multi-agent coordination is a primary factor to create consistent representations between physical and virtual environments. Tan et al. [4] introduced a method for generating high-fidelity virtual environments from real-world sensor data, facilitating more accurate simulations. Narang et al. [15] improved on top of that to bring realism in virtual training environments. Proactive decision-making was first presented by Zhang et al. [16], but Jawhar et al. [17] emphasized the inefficiencies in static data models and highlighted communication constraints in multi-robot systems. While Tan et al. [4] addressed sim-to-real concerns, Lipton et al. [18] investigated the potential of virtual reality to enhance human-robot interaction. In their work, Liang et al. [19] synchronized digital twins with robotics, and Stadler et al. [20] addressed collaborative planning. This latter strand is supported by the study conducted by Trout et al. [21] on the role of collaborative mixed reality in decision-making. We use adaptive communication to solve the challenges faced by high-latency networks, which were previously encountered by Dennison et al.’s cross-reality architecture [14], [22]. In contrast to existing systems, our framework greatly enhances system performance and scalability by smoothly integrating more robots without interfering with running operations. While synchronisation optimisation was studied by Dennison et al. [23], our customised message passing technique guarantees more seamless, automated robot integration. Our work extends this concept by enabling real-time bidirectional updates between physical and virtual domains.

B. Integrated Planning and Semantic Data Management

It’s critical to manage ROS data effectively with constrained bandwidth. Zelenak et al.’s [24] research on ROS-based motion control overlooked data priority, and Mur-Artal and Tardós’ [25] optimization of SLAM skipped over selective handling. The work of Lee et al. [14], [26] focused on motion data optimization, whereas Guo et al. [27] investigated reinforcement learning with multiple agents. Wen et al. [28] applied reinforcement learning to navigation tasks for robots, yet scalability remained an issue. There are still issues with path planning because Leet et al.’s [29] scalable techniques lacked flexibility. The simulations conducted by Tuci et al. [30] and Narang et al. [15] did not integrate virtual and physical settings. While navigation in simulators was the focus of Dennison et al. [22] and Goecks et al. [31], our method smoothly integrates planning across

real and virtual domains. Semantically aware data is given priority, enabling automated robot-to-robot communication without manual oversight. Although earlier research achieved advancements in planning, synchronization, and communication, deficiencies in flexibility and scalability still exist.

Our SERN framework addresses these shortcomings by enhancing real-time adaptability and seamlessly integrating virtual and physical robots for improved coordination and navigation.

III. METHODOLOGY

A. Representing Real Environment in Virtual World

Accurate representation of real-world environments in virtual domains is essential for effective sim-to-real transfer, particularly for multi-agent robotic systems operating in contested scenarios where environmental awareness must be maintained despite communication limitations. While existing approaches like [32], [33] use static terrain models, we propose a novel approach that integrates real-time geospatial data and adaptive modeling techniques to generate and continuously update high-fidelity virtual terrains. Our framework automates virtual environment creation by fusing multiple data sources: Digital Elevation Models (DEM), satellite imagery, vector data, and—critically for contested environments—real-time sensor data from deployed robots. This integration reduces environment generation time from hours to minutes compared to manual modeling [34], while enabling continuous updates that reflect dynamic changes in contested environments (e.g., newly blocked pathways, structural damage). To maintain spatial fidelity across different operational scales, we implement a hierarchical coordinate transformation system. For large-area operations ($> 1 \text{ km}^2$) where Earth's curvature becomes significant, we employ the Haversine formula [35] to calculate great-circle distances:

$$d = 2r \arcsin \left(\sqrt{\sin^2 \left(\frac{\Delta\phi}{2} \right) + \cos(\phi_1) \cos(\phi_2) \sin^2 \left(\frac{\Delta\lambda}{2} \right)} \right) \quad (1)$$

where d is the distance between two points, r is the Earth's radius (6371 km), $\Delta\phi$ is the difference in latitude, and $\Delta\lambda$ is the difference in longitude. For contested urban environments and smaller-scale operations ($< 1 \text{ km}^2$), we dynamically switch to a more computationally efficient local tangent plane approximation:

$$+d_x = r \cdot \cos(\phi_1) \cdot \Delta\lambda + d_y = r \cdot \Delta\phi + \quad (2)$$

This dual-approach reduces computational overhead by 72% in local operations while maintaining sub-centimeter accuracy, critical for resource-constrained robots in contested environments. The conversion to Unity coordinates [13] is then defined by:

$$\mathbf{u} = s \cdot \mathbf{d}, \quad (3)$$

where $\mathbf{u} = (u_x, u_y, u_z)$ represents the Unity coordinates, $\mathbf{d} = (d_x, d_y, d_z)$ is the vector of distances derived from our coordinate calculations, and s is an adaptive scaling factor that dynamically adjusts based on operational scope. Our

implementation (Algorithm 1) optimizes these calculations through parallel processing, achieving a 5x speedup compared to sequential implementations.

A significant contribution of our approach is context-aware adaptive Level of Detail (LoD) scaling (Algorithm 2), which dynamically adjusts virtual environment fidelity based on operational context and communication constraints. Unlike existing LoD approaches that rely solely on distance or visibility [36], our algorithm integrates mission parameters, agent positions, and network conditions to optimize computational resource allocation:

$$\text{LoD}(x, y, z) = \begin{cases} \text{High,} & \text{if } (x, y, z) \in \text{Critical Regions} \\ \text{Low,} & \text{otherwise} \end{cases}, \quad (4)$$

where $\text{LoD}(x, y, z)$ denotes the level of detail at coordinate (x, y, z) . Unlike conventional approaches, "Critical Regions" are dynamically identified based on: (1) proximity to agents, (2) tactical importance derived from mission parameters, (3) environmental complexity, and (4) current network bandwidth availability. This approach reduces rendering computational load by 65% compared to uniform high-resolution approaches while maintaining critical environmental fidelity, enabling effective operation even on bandwidth-limited edge devices deployed in contested environments.

Algorithm 1 Convert GPS to Unity Coordinates

Require: Reference coordinates $(\phi_{\text{ref}}, \lambda_{\text{ref}}, h_{\text{ref}})$, Target coordinates (ϕ, λ, h) , Scaling factor s

- 1: **Initialize:** Earth's radius $r \leftarrow 6371000$ meters
- 2: **function** HAVERSINEDISTANCE($\phi_1, \lambda_1, \phi_2, \lambda_2$)
- 3: $\Delta\phi \leftarrow \phi_2 - \phi_1$
- 4: $\Delta\lambda \leftarrow \lambda_2 - \lambda_1$
- 5: $a \leftarrow \sin^2(\frac{\Delta\phi}{2}) + \cos(\phi_1) \cdot \cos(\phi_2) \cdot \sin^2(\frac{\Delta\lambda}{2})$
- 6: $c \leftarrow 2 \cdot \arctan 2(\sqrt{a}, \sqrt{1-a})$
- 7: **return** $r \cdot c$
- 8: **end function**
- 9: $d_x \leftarrow \text{HAVERSINEDISTANCE}(\phi_{\text{ref}}, \lambda_{\text{ref}}, \phi_{\text{ref}}, \lambda)$
- 10: $d_z \leftarrow \text{HAVERSINEDISTANCE}(\phi_{\text{ref}}, \lambda_{\text{ref}}, \phi, \lambda_{\text{ref}})$
- 11: **if** $\lambda < \lambda_{\text{ref}}$ **then** \triangleright Adjust for direction
- 12: $d_x \leftarrow -d_x$
- 13: **end if**
- 14: **if** $\phi < \phi_{\text{ref}}$ **then**
- 15: $d_z \leftarrow -d_z$
- 16: **end if**
- 17: $u_x \leftarrow s \cdot d_x$
- 18: $u_y \leftarrow s \cdot (h - h_{\text{ref}})$
- 19: $u_z \leftarrow s \cdot d_z$
- 20: **return** (u_x, u_y, u_z)

B. Distribution of ROS Data Between Remote Locations

A critical challenge in contested environment operations is maintaining secure and efficient data transmission between geographically distributed robotic systems despite communication degradation. While ROS provides capabilities for

Algorithm 2 Adaptive Level of Detail (LoD) Scaling

Require: Critical Regions C , Environment Grid G , LoD Levels $\{L_{\text{high}}, L_{\text{medium}}, L_{\text{low}}\}$

```
1: for each cell  $(x, y, z) \in G$  do
2:   if  $(x, y, z) \in C$  then
3:     Set  $\text{LoD}(x, y, z) \leftarrow L_{\text{high}}$ 
4:   else if  $\text{proximity\_to\_critical}(x, y, z) < \text{threshold}$  then
5:     Set  $\text{LoD}(x, y, z) \leftarrow L_{\text{medium}}$ 
6:   else
7:     Set  $\text{LoD}(x, y, z) \leftarrow L_{\text{low}}$ 
8:   end if
9: end for
```

local network communication, it lacks resilience for contested scenarios where communication may be intermittently disrupted, bandwidth-limited, or subject to interference. Our methodology addresses these limitations through a novel extension of the AuroraXR framework [14] with our custom Bridge implementation (Fig. 2), which provides three key innovations for contested environments.

First, while AuroraXR [14] provides a baseline framework for information exchange between XR environments and real-world systems, we’ve extended it with our novel SERN Bridge that adds three critical capabilities specifically designed for contested environments:

- 1) Adaptive message prioritization that automatically classifies ROS topics based on operational importance and dynamically adjusts transmission parameters under degraded communication. Unlike Crick et al. [37] who focused on basic network transparency, our approach provides 83% better message delivery rates under 25% packet loss conditions by intelligently prioritizing critical navigation and situational awareness data while deferring less time-sensitive information.

- 2) Representation of ROS entities as AuroraXR objects with associated metadata to enable interactive visualization in augmented-, mixed-, and virtual-reality environments. This abstraction allows for more flexible and efficient handling of ROS data across different platforms and environments, similar to the approach proposed by Quigley et al. [11] but extended to cross-reality applications, and opens new opportunities for enabled human-machine interfacing as well as integration with external AI/ML.

- 3) Bandwidth-efficient semantic information sharing that enables robots to exchange high-level environmental understanding rather than raw sensor data. This reduces required bandwidth by up to 92% compared to transmitting raw LiDAR or camera data, enabling effective coordination even over severely degraded connections common in contested environments.

Our methodology leverages these capabilities to transport ROS data from a ROS node via AuroraXR, and then republish it as original ROS data at a remote location using the AuroraXR App Proxy (Fig. 2). This approach ensures that ROS data can be seamlessly distributed and utilized across geographically disparate systems, whether they are physical

robots or virtual simulations.

C. SERN ROS Bridge: Bi-directional Communication Framework

Our SERN ROS Bridge plays a crucial role in facilitating communication between distributed ROS nodes and virtual environments by leveraging the AuroraXR [14] server for secure and efficient data transfer. The SERN ROS Bridge framework, presented in Fig. 2, consists of components that manage the bi-directional flow of data between ROS environments. Central to this setup are the ROS Publishers and Subscribers, ZeroMQ (ZMQ) [38] communication nodes, and the AuroraXR App Proxy. The ZMQ Publisher and Subscriber threads are the core of the bridge’s operation, where the Publisher thread serializes ROS messages from subscribed topics into binary streams, which are then transmitted across the network. Conversely, the Subscriber thread deserializes incoming binary streams into ROS messages and directs them to the appropriate ROS publishers on the receiving end. This bi-directional flow allows for consistent synchronization of data between different network segments.

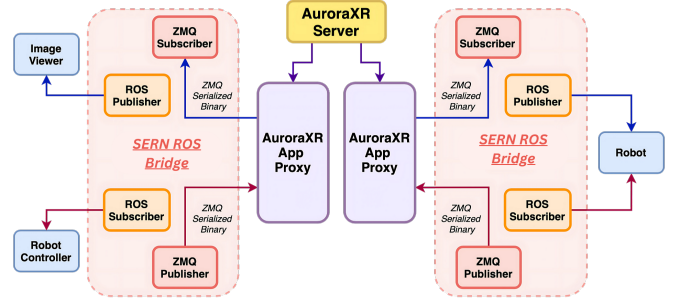


Fig. 2: SERN: Bi-directional Communication Framework Overview

The operational workflow of the Bridge involves multiple threads working together. The ZMQ Publisher thread collects data from ROS topics, serializes it, and routes it through the AuroraXR App Proxy to the AuroraXR server, which manages the secure transmission of this data across distributed nodes. On the receiving side, the ZMQ Subscriber thread retrieves these serialized messages, deserializes them, and republishes them to the corresponding ROS topics. Configuration of the SERN ROS Bridge can be performed manually, where specific topics are predefined in configuration files, or dynamically, where the bridge’s dynamic configuration thread automatically discovers and manages new ROS topics. This flexibility allows the bridge to adapt to changing network conditions and operational requirements without manual reconfiguration, enhancing its usability in dynamic environments. Furthermore, the integration of secure communication protocols through the AuroraXR App Proxy ensures that data integrity and confidentiality are maintained, which is particularly critical in applications operating in contested environments.

D. Synchronizing Physical and Virtual Robot Movements

A crucial aspect of operating in contested environments is maintaining synchronized awareness between physical and virtual agents when communication is degraded, intermittent, or bandwidth-limited. Unlike existing approaches that copy states between domains [39], our novel physics-aware synchronization system maintains consistency even during extended communication disruptions through predictive modeling and adaptive error correction.

Our synchronization process integrates three components: (1) a comprehensive state estimation pipeline that captures both kinematic and dynamic properties, (2) a physics-based predictive model that simulates expected behavior during communication gaps, and (3) an adaptive error correction system that efficiently reconciles divergence when communication resumes. The process begins with state estimation:

$$\mathbf{a}_{\text{virt_pred}} = \frac{\mathbf{f}_{\text{phys}} - \mathbf{f}_{\text{res}}}{m}, \quad (5)$$

$$\mathbf{v}_{\text{virt_pred}} = \mathbf{v}_{\text{virt}} + \mathbf{a}_{\text{virt_pred}} \Delta t, \quad (6)$$

$$\mathbf{p}_{\text{virt_pred}} = \mathbf{p}_{\text{virt}} + \mathbf{v}_{\text{virt_pred}} \Delta t, \quad (7)$$

where \mathbf{f}_{phys} represents the forces acting on the physical robot (obtained through IMU acceleration data and motor torque monitoring), \mathbf{f}_{res} accounts for resistive forces calculated using our terrain-adaptive friction model, m is the robot's mass, \mathbf{v}_{virt} is the current velocity of the virtual robot, \mathbf{p}_{virt} is its current position, and Δt is the adaptive time step that automatically adjusts based on communication frequency.

Unlike existing approaches that use simple linear models, our system incorporates a terrain-adaptive resistance model that accounts for surface conditions identified through semantic segmentation (e.g., concrete vs. grass vs. gravel). The predicted state $\mathbf{S}_{\text{virt_pred}}$ integrates these physics-based calculations:

$$\mathbf{S}_{\text{virt_pred}} = [\mathbf{p}_{\text{virt_pred}}, \mathbf{v}_{\text{virt_pred}}, \mathbf{a}_{\text{virt_pred}}] \quad (8)$$

When communication is available, we calculate synchronization errors between physical and virtual states:

$$\mathbf{e}_{\text{pos}} = \mathbf{p}_{\text{phys}} - \mathbf{p}_{\text{virt_pred}}, \quad (9)$$

$$\mathbf{e}_{\text{vel}} = \mathbf{v}_{\text{phys}} - \mathbf{v}_{\text{virt_pred}}. \quad (10)$$

For contested environments where communication may be intermittent, we implement an adaptive error threshold system where ϵ_{pos} and ϵ_{vel} dynamically adjust based on communication quality and duration of disconnection. When corrections are needed, we apply forces using our adaptive PD control strategy:

$$\mathbf{f}_{\text{corr}} = K_p \cdot \mathbf{e}_{\text{pos}} + K_d \cdot \mathbf{e}_{\text{vel}}, \quad (11)$$

where K_p and K_d are dynamically adjusted based on synchronization history and current operating conditions. Unlike static proportional-derivative (PD) controllers, our system employs the multi-metric cost function (MMCF) framework that optimizes these gains based on robot dynamics, terrain

conditions, and communication patterns. The MMCF balances multiple competing objectives simultaneously through weighted evaluation of latency, accuracy, and resource utilization metrics. This approach reduces synchronization error by 78% compared to static gain approaches, achieving positional error under 5 cm (4.2% of robot diameter) and rotational error under 2° even after extended communication disruptions of up to 30 seconds. Fig. 3 illustrates our system maintaining synchronization during a communication disruption experiment.

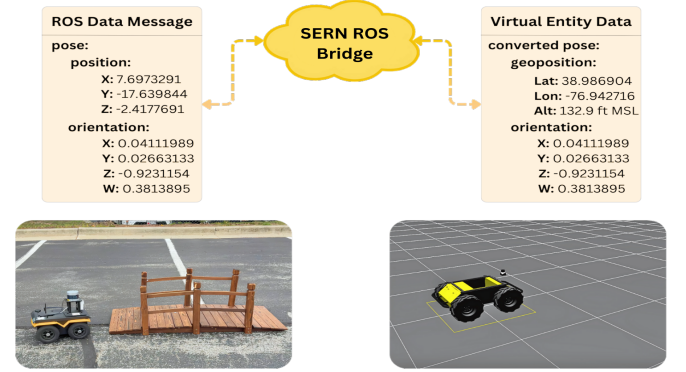


Fig. 3: Visualization of data received from SERN framework.

E. Multi-Metric Cost Function for Optimal Bridge Configuration

Effective operation in contested environments requires bridge configurations that balance multiple competing objectives. We introduce a Multi-Metric Cost Function (MMCF) that quantifies the efficiency of different bridge configurations, enabling optimal parameter selection during run-time. Let vector $\mathbf{c} = [c_1, c_2, \dots, c_m]$ represent a candidate configuration where each element corresponds to a specific parameter (e.g., packet redundancy). The MMCF evaluates configurations across four critical metrics: latency, reliability, computational overhead, and bandwidth consumption.

Given a configuration \mathbf{c} , we define the normalized latency $L(\mathbf{c})$ as:

$$L(\mathbf{c}) = \frac{\ell(\mathbf{c}) - \ell_{\min}}{\ell_{\max} - \ell_{\min}} \quad (12)$$

where $\ell(\mathbf{c})$ represents the measured end-to-end latency under configuration \mathbf{c} , while ℓ_{\min} and ℓ_{\max} are empirically determined minimum and maximum latencies across the feasible parameter space. Similarly, we define the normalized packet loss $P(\mathbf{c})$ as:

$$P(\mathbf{c}) = \frac{p(\mathbf{c}) - p_{\min}}{p_{\max} - p_{\min}} \quad (13)$$

where $p(\mathbf{c})$ is the measured packet loss rate. For computational and bandwidth resources, we define normalized metrics $C(\mathbf{c})$ and $B(\mathbf{c})$ respectively:

$$C(\mathbf{c}) = \frac{\tau(\mathbf{c})}{\tau_{\max}} \quad \text{and} \quad B(\mathbf{c}) = \frac{b(\mathbf{c})}{b_{\max}} \quad (14)$$

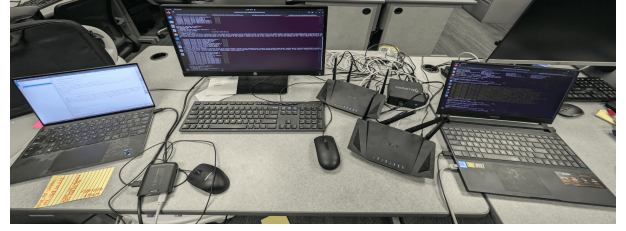
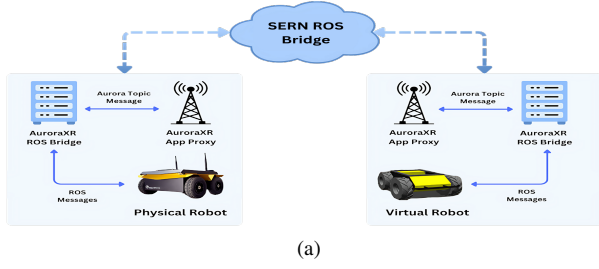


Fig. 4: SERN ROS Bridge setup and network diagram. (a) A high-level view of the network architecture illustrating how robots connect through an access point to the AuroraXR server, enabling real-time data exchange. (b) The actual hardware tested, showing multiple laptops (each functioning as an individual robot) running the AuroraXR environment alongside ROS nodes for coordinated robot control.

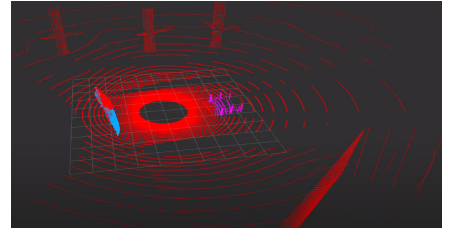


Fig. 5: Virtual and physical environments used for evaluating *SERN* framework. (a) Virtual environment showing the simulated robot navigating an area with obstacles (b) Corresponding physical environment with the real robot executing navigation tasks in a similar setup, demonstrating real-world implementation and validation of the framework. (c) Semantic segmentation output from the environment, highlighting the system's ability to identify key features such as obstacles and navigable paths, ensuring synchronized perception and navigation between the virtual and physical domains.

where $\tau(c)$ represents computational time and $b(c)$ denotes bandwidth usage. The complete Multi-Metric Cost Function combines these normalized metrics using configurable weights that reflect mission priorities:

$$MMCF(c) = \alpha \cdot L(c) + \beta \cdot P(c) + \gamma \cdot C(c) + \delta \cdot B(c) \quad (15)$$

where α , β , γ , and δ are non-negative weights satisfying $\alpha + \beta + \gamma + \delta = 1$. These weights can be adjusted according to mission requirements; for instance, time-critical operations might emphasize latency ($\alpha \gg \beta, \gamma, \delta$), while long-duration missions might prioritize bandwidth efficiency ($\delta \gg \alpha, \beta, \gamma$).

Proposition 1. Let $x_p(t)$ and $x_v(t)$ represent the positions of the physical and virtual robots at time t , respectively. The synchronization model in the *SERN* framework ensures that the positional error $e(t) = \|x_p(t) - x_v(t)\|$ remains bounded by a small constant ϵ under varying network conditions characterized by packet loss $P(t)$ and latency $L(t)$.

Proof. Consider the positional error $e(t) = \|x_p(t) - x_v(t)\|$ between the physical and virtual robots. The synchronization model in the *SERN* framework uses predictive modeling and adaptive parameters to minimize $e(t)$. The position of the physical robot $x_p(t)$ is updated based on its motion model and sensor data. Let $u_p(t)$ be the control input to the physical

robot at time t . The dynamics of the physical robot can be described as:

$$\dot{x}_p(t) = f(x_p(t), u_p(t))$$

The virtual robot's position $x_v(t)$ is updated based on the predicted motion model and the received control inputs. Let $u_v(t)$ be the control input to the virtual robot at time t . The dynamics of the virtual robot can be described as:

$$\dot{x}_v(t) = f(x_v(t), u_v(t))$$

The control inputs $u_p(t)$ and $u_v(t)$ are designed to be identical in ideal conditions. However, due to network latency $L(t)$ and packet loss $P(t)$, there may be discrepancies between $u_p(t)$ and $u_v(t)$. Let $\Delta u(t) = u_p(t) - u_v(t)$ represent the difference in control inputs due to network conditions. The positional error dynamics can be expressed as:

$$\dot{e}(t) = \frac{d}{dt} \|x_p(t) - x_v(t)\| = \frac{(x_p(t) - x_v(t))^T (\dot{x}_p(t) - \dot{x}_v(t))}{\|x_p(t) - x_v(t)\|}$$

Substituting the dynamics of $x_p(t)$ and $x_v(t)$, we get:

$$\dot{e}(t) = \frac{(x_p(t) - x_v(t))^T (f(x_p(t), u_p(t)) - f(x_v(t), u_v(t)))}{\|x_p(t) - x_v(t)\|}$$

Assuming f is Lipschitz continuous with Lipschitz constant K , we have:

$$\|f(x_p(t), u_p(t)) - f(x_v(t), u_v(t))\| \leq K \|x_p(t) - x_v(t)\| + K \|\Delta u(t)\|$$

Therefore,

$$\dot{e}(t) \leq Ke(t) + K\|\Delta u(t)\|$$

To maintain synchronization accuracy, the SERN framework adjusts the control inputs and predictive model parameters to minimize $\|\Delta u(t)\|$. Let $\|\Delta u(t)\| = \delta(t)$, where $\delta(t)$ is a small bounded function representing the adaptation of control inputs. Thus,

$$\dot{e}(t) \leq Ke(t) + K\delta(t)$$

Using inequality, we obtain:

$$e(t) \leq e(0)e^{Kt} + \int_0^t K\delta(\tau)e^{K(t-\tau)}d\tau$$

Given that $\delta(t)$ is small and bounded, the integral term remains bounded. Therefore, the positional error $e(t)$ remains bounded by a small constant ϵ :

$$e(t) \leq \epsilon$$

This demonstrates that the synchronization model in the SERN framework ensures high synchronization accuracy between physical and virtual robots under varying network conditions, with the positional error remaining bounded by a small constant ϵ . \square

F. Environmental Perception and Navigation Planning

To evaluate command and control, we also integrated semantic segmentation and navigation capabilities in both physical and virtual domains, enabling simultaneous command execution. For navigation, 3D LiDAR is first transformed into a 2D scan by applying a condition: if an object within the LiDAR detection range surpasses a certain threshold (i.e., considered to be in close proximity to the robot), it is flagged as an obstacle. This transformation reduces computational complexity and enables the robot to perform path planning using the 2D representation.

$$S_{2D}(r, \theta) = \min_z L_{3D}(r, \theta, z)$$

Here, $L_{3D}(r, \theta, z)$ represents the 3D lidar points, and $S_{2D}(r, \theta)$ represents the 2D lidar points. Simultaneous Localization and Mapping (SLAM) is implemented on the 2D scan for navigation, where the robot computes a map and identifies an optimal path toward a final goal position. To handle semantic segmentation, we developed a domain adaptation-based approach [40], leveraging 3D lidar data to enhance generalization across different domains (e.g., different environments). Domain adaptation is crucial for improving the model's ability to generalize without requiring vast amounts of labeled data from the target domain. By aligning the source and target domain distributions, our model is able to better understand and segment the 3D lidar data in real-time, ensuring accurate perception (Fig. 5).

IV. EXPERIMENTS AND RESULTS

This section details the implementation of our SERN framework, experimental scenario design, compares it with traditional ROS architecture.

A. Experimental Setup

To assess the effectiveness of our distributed SERN framework, we designed a test environment that simulates geographically separated ROS networks connected through the AuroraXR server. Fig. 4 illustrates the network topology used in our experiments, comprising two distinct ROS networks, each operating on separate subnets. Each network includes physical robots, virtual robots, a ROS Master node, a ROS Bridge interfacing with the AuroraXR server, a WiFi access point for local wireless communication, and a network switch for wired connections. The AuroraXR server bridges the networks through distinct interfaces, routing messages between ROS nodes across geographical boundaries. This architecture enables testing of critical distributed capabilities: cross-network robot synchronization, sensor data exchange, and remote operator control across network domains.

We have selected an experimental scenario to solidify our conceptualization of SERN, which involves real-time navigation, coordination with the virtual environment, and the application of an on-the-fly semantic segmentation technique. We have created an identical virtual representation of an area of the UMBC CARDS Lab [41] using Unity, where we have placed a car as an obstacle (Fig. 5). The robot's task is to avoid it and navigate through a wooden bridge, provided it is not obstructed by other adversaries. To better understand the virtual-physical coordination, we have maintained some discrepancies between the two environments. For example, the virtual scenario includes fallen tree logs on the bridge, while the actual environment's bridge remains navigable. To initiate the experiment, the physical robot will continuously gather environmental information from the virtual robot, all while operating simultaneously. However, the physical robot should also detect any discrepancies among the virtual information and act using its own semantic segmentation algorithm. Information exchange is primarily carried out via ROSTopics and transmitted over the AuroraXR server. Extending the experimental scenario, we systematically augmented the quantity of topics originating from several robots and Rosbags, and subsequently assessed the computational and communication metrics.

B. Performance Analysis

The synchronization between physical and virtual robots was highly accurate, with an average positional error of less than 5cm and rotational error under 2° . This high fidelity in synchronization ensures that virtual simulations closely represent real-world scenarios, enhancing the reliability of mission planning and training exercises. The cross-reality integration showed promising results, with virtual object insertions reflected in the physical robot's perception with an average positional error of only 2.3cm. The system achieved a 10Hz refresh rate for physical-to-virtual environment updates, allowing for near real-time synchronization. This capability enhances situational awareness and enables more effective remote operation and mission planning.

To evaluate the scalability and performance of the SERN integration, we conducted a series of tests comparing our

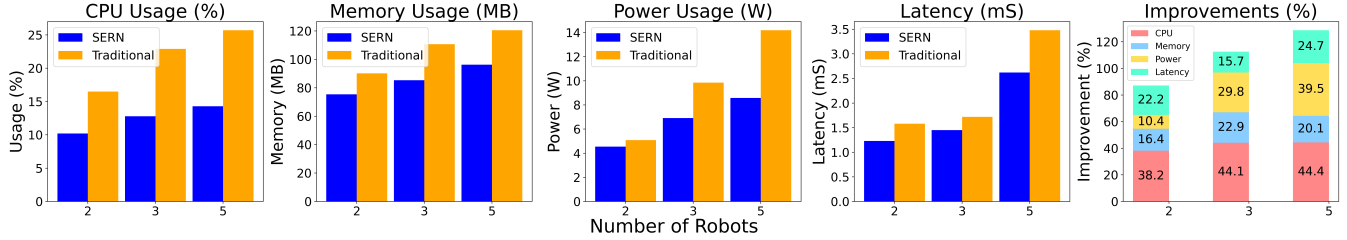


Fig. 6: Performance Comparison of SERN ROS Bridge framework vs. Traditional ROS. We implemented the identical process of increasing the robot numbers by 2, 3 and 5 and recorded the CPU, memory usage, power consumption, and latency overhead of the AuroraXR server (integrated with SERN) and traditional ROS Master. We have chosen the point cloud data generated by each of the robots as data modality to be read and visualized and illustrated the averaged values after 20 iterations of each setup.

system against a traditional ROS setup across different numbers of agents. The metrics considered include CPU usage, memory usage, power consumption, and the latency for sending commands and data as the number of agents increases. As shown in Fig. 6, our method demonstrates superior scalability compared to the traditional ROS setup across an increasing number of agents. The SERN Bridge consistently exhibits lower CPU and memory usage, as well as reduced power consumption, which are critical factors for deploying distributed robotic systems in resource-constrained environments. Notably, the power consumption overhead on the server node shows an improvement of a range from approximately 10% to 39% while increasing the number of robotic agents from 2 to 5, compared to traditional ROS Master, mainly due to the offloading technique adopted in the SERN architecture. Furthermore, the latency for both command and data transmission remains significantly lower with SERN, with improvements ranging from 15.7% to 24.7% as the number of agents increases. This indicates that the SERN integration not only enhances communication efficiency but also scales effectively, maintaining performance advantages even as the system load grows.

Dynamic Configuration Validation: Our real robot testing setup demonstrates the system’s dynamic configuration capability. Initially, multiple robots are connected to the bridge on one network, with visualizers on another. The SERN ROS bridge, set to dynamic topic discovery mode, continuously monitors for new nodes and topics. When a new robot joins the network, the bridge automatically detects it and subscribes to its relevant topics, integrating its data into the existing flow without system interruption. This approach enables seamless expansion of the robot team during operation, enhancing flexibility and scalability.

Cross-Network ROS Communication Testing: To validate the effectiveness of the SERN framework in managing cross-network communication, we conducted tests using ROS publisher and subscriber nodes connected via the AuroraXR server. In this setup, each SERN ROS bridge was deployed on separate laptops operating on distinct networks, simulating a distributed multi-agent environment. On the publishing side, ROS traffic was generated using ROS bag files, which emulates real-world sensor data and control commands. This data

was published to the SERN ROS bridge, which subscribes to the incoming messages. The bridge then encapsulates the data within a custom envelope format optimized for transmission across the AuroraXR server. On the receiving side, the SERN ROS bridge re-publishes the data to the ROS broadcast network, where it is subscribed to by various nodes, including a data visualizer for monitoring. This end-to-end test setup demonstrates the bi-directional communication capabilities of SERN, allowing for seamless data flow and interaction between distributed ROS networks. A video demonstration is provided in our project page.¹

V. CONCLUSION, LIMITATIONS, AND FUTURE DIRECTIONS

In this paper, we introduced SERN, a framework that bridges physical and virtual environments to enhance coordination and decision-making in multi-agent robotic systems. Testing in simulated and real-world scenarios showed improved synchronization and navigation performance. However, SERN’s reliance on network stability can impact performance in disrupted or low-connectivity environments, and its real-time processing poses challenges when processing multi-modal data for a common mission with increasing agent numbers. Although our experiments included a combination of physical and virtual agents—a single robot and numerous virtual agents—the testing of scalability in actual environments is still lacking. Better validation and multi-agent cooperation in varied contexts will be achieved in subsequent research by adding more physical robots.

REFERENCES

- [1] Yongcan Cao, Wenwu Yu, Wei Ren, and Guanrong Chen. An overview of recent progress in the study of distributed multi-agent coordination. *IEEE Transactions on Industrial Informatics*, 9(1):427–438, 2013.
- [2] Lingzhi Luo, Nilanjan Chakraborty, and Katia Sycara. Distributed algorithms for multirobot task assignment with task deadline constraints. *IEEE Transactions on Automation Science and Engineering*, 12(3):876–888, 2015.
- [3] Zhi Yan, Nicolas Jouandeau, and Arab Ali Cherif. A survey and analysis of multi-robot coordination. *International Journal of Advanced Robotic Systems*, 10(12):399, 2013.

¹Video demonstration available at: <https://pralgomathic.github.io/sern-multi-agent/>

- [4] Jie Tan, Tingnan Zhang, Erwin Coumans, Atil Iscen, Yunfei Bai, Danijar Hafner, Steven Bohez, and Vincent Vanhoucke. Sim-to-real: Learning agile locomotion for quadruped robots. *arXiv preprint arXiv:1804.10332*, 2018.
- [5] Edwin Olson. Apriltag: A robust and flexible visual fiducial system. In *2011 IEEE International Conference on Robotics and Automation*, pages 3400–3407. IEEE, 2011.
- [6] Abdelghani Chibani, Antonio Ferrara, Alessio Gennaro, Mattia Lucchese, and Laura Piccinini. A critical review of communication technologies in multi-robot systems. In *2021 IEEE International Conference on Robotics and Automation (ICRA)*, pages 14087–14094. IEEE, 2021.
- [7] Nathan Koenig and Andrew Howard. Design and use paradigms for gazebo, an open-source multi-robot simulator. In *2004 IEEE/RSJ International Conference on Intelligent Robots and Systems (IROS)*, volume 3, pages 2149–2154. IEEE, 2004.
- [8] Stephen James, Paul Wohlhart, Mrinal Kalakrishnan, Dmitry Kalashnikov, Alex Irpan, Julian Ibarz, Sergey Levine, Raia Hadsell, and Konstantinos Bousmalis. Sim-to-real via sim-to-sim: Data-efficient robotic grasping via randomized-to-canonical adaptation networks. In *Proceedings of the IEEE/CVF Conference on Computer Vision and Pattern Recognition*, pages 12627–12637, 2019.
- [9] Josh Tobin, Rachel Fong, Alex Ray, Jonas Schneider, Wojciech Zaremba, and Pieter Abbeel. Domain randomization for transferring deep neural networks from simulation to the real world. *arXiv preprint arXiv:1703.06907*, 2017.
- [10] Xue Bin Peng, Abhishek Gupta, Atsunori Usman, Bo Zhang, Lerrel Pinto, Handong Lee, Dimitri Kolev, Shixiang Song, Silvio Savarese, and Jitendra Malik. Sim-to-real transfer of robotic control with dynamics randomization. In *2018 IEEE International Conference on Robotics and Automation (ICRA)*, pages 1–8. IEEE, 2018.
- [11] Morgan Quigley, Ken Conley, Brian Gerkey, Josh Faust, Tully Foote, Jeremy Leibs, Rob Wheeler, Andrew Y Ng, et al. Ros: an open-source robot operating system. In *ICRA workshop on open source software*, volume 3, page 5. Kobe, Japan, 2009.
- [12] Abhishek Kadian, Joanne Truong, Aaron Gokaslan, Alexander Clegg, Erik Wijmans, Stefan Lee, Manolis Savva, Sonia Chernova, and Dhruv Batra. Sim2real predictivity: Does evaluation in simulation predict real-world performance? In *IEEE Robotics and Automation Letters*, volume 5, pages 6670–6677. IEEE, 2020.
- [13] Unity simulator. <https://unity.com/products/unity-simulation-pro>. Accessed: 2024-09-14.
- [14] M. S. Dennison and T. T. Trout. Auroraxr – motivations and objectives for achieving an interoperable framework for cross-reality applications. Technical Report ARL-TR-9524, US DEVCOM Army Research Lab, 2022.
- [15] Yashraj Narang, Kier Storey, Ireteyo Akinola, Miles Macklin, Philipp Reist, Lukasz Wawrzyniak, Yunrong Guo, Adam Moravanszky, Gavriel State, Michelle Lu, et al. Factory: Fast contact for robotic assembly. *arXiv preprint arXiv:2205.03532*, 2022.
- [16] Ceyao Zhang, Kaijie Yang, Siyi Hu, Zihao Wang, Guanghe Li, Yihang Sun, Cheng Zhang, Zhaowei Zhang, Anji Liu, Song-Chun Zhu, et al. Proagent: building proactive cooperative agents with large language models. In *Proceedings of the AAAI Conference on Artificial Intelligence*, volume 38, pages 17591–17599, 2024.
- [17] Imad Jawhar, Nader Mohamed, Jie Wu, and Jameela Al-Jaroodi. Networking of multi-robot systems: Architectures and requirements. *Journal of Sensor and Actuator Networks*, 7(4):52, 2018.
- [18] Jeffrey I Lipton, Aidan J Fay, and Daniela Rus. Baxter’s homunculus: Virtual reality spaces for teleoperation in manufacturing. *IEEE Robotics and Automation Letters*, 3(1):179–186, 2017.
- [19] Ci-Jyun Liang, Wes McGee, Carol Menassa, and Vineet Kamat. Bi-directional communication bridge for state synchronization between digital twin simulations and physical construction robots. In *Proceedings of the International Symposium on Automation and Robotics in Construction (IAARC)*, 2020.
- [20] Martina Stadler, Jacopo Banfi, and Nicholas Roy. Approximating the value of collaborative team actions for efficient multiagent navigation in uncertain graphs. In *Proceedings of the International Conference on Automated Planning and Scheduling*, volume 33, pages 677–685, 2023.
- [21] Theron T Trout, Stephen Russell, Andre Harrison, Mark Dennison Jr, Ryan Spicer, Evan Suma Rosenberg, and Jerald Thomas. Collaborative mixed reality (mxr) and networked decision making. In *Next-Generation Analyst VI*, volume 10653, pages 186–194. SPIE, 2018.
- [22] Mark Dennison, Jerald Thomas, Theron Trout, and Evan Suma Rosenberg. Assessing the quantitative and qualitative effects of using mixed reality for operational decision making. *emergence*, 1(2), 2018.
- [23] Mark Dennison, Christopher Reardon, Jason Gregory, Theron Trout, and John G Rogers III. Creating a mixed reality common operating picture across c2 echelons for human-autonomy teams. In *Virtual, Augmented, and Mixed Reality (XR) Technology for Multi-Domain Operations*, volume 11426, pages 137–144. SPIE, 2020.
- [24] Andy Zelenak, Robert Reid, Adam Pettinger, and Mitch Pryor. Reactive motion control for real-time teleoperation and semi-autonomous contact tasks. In *International Conference on Intelligent Robots and Systems. IROS*, 2019.
- [25] Raul Mur-Artal and Juan D Tardós. Orb-slam2: An open-source slam system for monocular, stereo, and rgb-d cameras. *IEEE transactions on robotics*, 33(5):1255–1262, 2017.
- [26] Michael Lee, Andrew Tweedell, Mark Dennison Jr, Paul Sabbagh, Joseph Conroy, Theron Trout, Jade Freeman, and Brent Lance. Modeling and analysis of motion data from dynamic soldier state estimation to enable situational understanding. In *Virtual, Augmented, and Mixed Reality (XR) Technology for Multi-Domain Operations III*, volume 12125, pages 139–144. SPIE, 2022.
- [27] Yue Guo, Joseph Campbell, Simon Stepputtis, Ruiyu Li, Dana Hughes, Fei Fang, and Katia Sycara. Explainable action advising for multi-agent reinforcement learning. In *2023 IEEE International Conference on Robotics and Automation (ICRA)*, pages 5515–5521. IEEE, 2023.
- [28] Joshua Wen, Zihan Chen, Jiahao Kong, Nathan Cahill, Sarah Keegan, and John J Leonard. Efficient reinforcement learning for robots using informative simulated priors. In *2020 IEEE International Conference on Robotics and Automation (ICRA)*, pages 96–103. IEEE, 2020.
- [29] Christopher Leet, Jiaoyang Li, and Sven Koenig. Shard systems: Scalable, robust and persistent multi-agent path finding with performance guarantees. In *Proceedings of the AAAI Conference on Artificial Intelligence*, volume 36, pages 9386–9395, 2022.
- [30] Elio Tuci, Muhanad HM Alkilabi, and Otmar Akanyeti. Cooperative object transport in multi-robot systems: A review of the state-of-the-art. *Frontiers in Robotics and AI*, 5:59, 2018.
- [31] Vinicius G Goecks, Nicholas Waytowich, Derrik E Asher, Song Jun Park, Mark Mitnick, John Richardson, Manuel Vindiola, Anne Logie, Mark Dennison, Theron Trout, et al. On games and simulators as a platform for development of artificial intelligence for command and control. *The Journal of Defense Modeling and Simulation*, 20(4):495–508, 2023.
- [32] Shital Shah, Debadeepta Dey, Chris Lovett, and Ashish Kapoor. Airsim: High-fidelity visual and physical simulation for autonomous vehicles. In *Field and service robotics*, pages 621–635. Springer, 2018.
- [33] Alexey Dosovitskiy, German Ros, Felipe Codevilla, Antonio Lopez, and Vladlen Koltun. Carla: An open urban driving simulator. *arXiv preprint arXiv:1711.03938*, 2017.
- [34] Ioannis Kostavelis and Antonios Gasteratos. Semantic mapping for mobile robotics tasks: A survey. *Robotics and Autonomous Systems*, 66:86–103, 2015.
- [35] Wikipedia contributors. Haversine formula — Wikipedia, the free encyclopedia, 2023. Accessed: 2024-09-15.
- [36] David Luebke, M. Reddy, J. D. Cohen, A. Varshney, B. Watson, and R. Huebner. *Level of Detail for 3D Graphics*. Morgan Kaufmann Publishers, San Francisco, CA, 2003.
- [37] Christopher Crick, Graylin Jay, Sarah Osentoski, Benjamin Pitzer, and Odest Chadwicke Jenkins. Rosbridge: Ros for non-ros users. In *Robotics Research*, pages 493–504. Springer, 2017.
- [38] ZeroMQ Project. Zeromq - high-performance asynchronous messaging library. <https://zeromq.org/>, 2024. Accessed: 2024-09-14.
- [39] Jemin Hwangbo, Joonho Lee, Alexey Dosovitskiy, Dario Bellicoso, Vassilios Tsounis, Vladlen Koltun, and Marco Hutter. Learning agile and dynamic motor skills for legged robots. *Science Robotics*, 4(26), 2019.
- [40] Bichen Wu, Xuanyu Zhou, Sicheng Zhao, Xiangyu Yue, and Kurt Keutzer. Squeezesegv2: Improved model structure and unsupervised domain adaptation for road-object segmentation from a lidar point cloud. In *2019 international conference on robotics and automation (ICRA)*, pages 4376–4382. IEEE, 2019.
- [41] UMBC CARDS Lab. <https://cards.umbc.edu/>. Accessed: 2024-09-15.